Magnetic Assembly of Superparamagnetic Iron Oxide Nanoparticle Clusters into Nanochains and Nanobundles

Slavko Kralj*,†,‡ and Darko Makovec†

†Department for Materials Synthesis, Jožef Stefan Institute, Jamova 39, 1000 Ljubljana, Slovenia and ‡Nanos SCI, Nanos Scientificae d.o.o., Teslova 30, 1000 Ljubljana, Slovenia

ABSTRACT We report on the syntheses of magnetoresponsive, superparamagnetic nanostructures with highly anisotropic shapes, *i.e.*, nanochains of controlled length and their bundles (nanobundles). These nanochains and nanobundles were obtained by the simultaneous magnetic assembly of superparamagnetic nanoparticle clusters (SNCs) and the fixation of the assembled SNCs with an additional layer of deposited silica, produced by a sol–gel process. This low-cost approach provides excellent length control of the short nanochains (approximately 6 or 14 SNCs per nanochain) and fine-tuning of the spacing between the neighboring SNCs inside an individual nanochain. Our magnetically responsive superparamagnetic nanostructures have a controlled aspect ratio, a uniform size, and a well-defined shape, and they express good colloidal stability. This general approach should lead to new, advanced applications of the nanochains and nanobundles in the treatment of cancer and in the ability to magnetically manipulate liquid and photonic crystals.

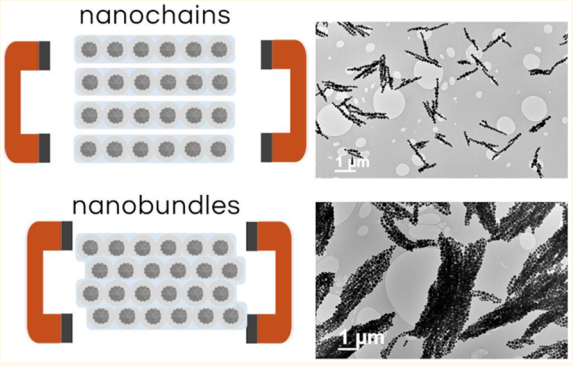

KEYWORDS: directed assembly · dynamic magnetic assembly · iron oxide nanochains · nanoparticle clusters · nanobundles · nanostructures

Colloidal particles with strong magnetic moments are of special interest for many applications where a large magnetic response is required.[1−4] Such applications include the magnetic carriers used for the separation of biomolecules from complex media, magnetically targeted drug-delivery systems,[5−8] and the building blocks for magnetically tunable photonic crystals.[9−11] Organizing magnetic nanoparticles into complex hierarchical structures in a template-free manner is a particularly challenging task.[12] Frequently, superparamagnetic nanoparticles (SNPs) with sizes below ~20 nm have been considered for such applications. Unlike the larger ferromagnetic particles, these SNPs do not agglomerate in a suspension as a result of the attractive magnetic dipole–dipole interactions and, therefore, can form stable colloids.[13] However, due to the small size required to achieve the superparamagnetic state, the individual SNPs have only small magnetic moments, which are frequently too small to allow for effective magnetic manipulation.[14,15] As the magnetization is fixed by the choice of the magnetic material—most commonly, inexpensive and nontoxic magnetic iron oxide is used—this means the magnetic moment largely depends on the size of nanoparticles. In order to improve the magnetic response while maintaining the superparamagnetic state of the colloidal particles, various self-assembly strategies have been employed to assemble the individual SNPs into superparamagnetic nanoparticle clusters (SNCs).[6,16−19] After the assembly, the nanoparticle clusters are usually coated with a layer of silica in order to improve the structural stability. Such SNCs in a colloidal suspension exhibit a strong response to an external magnetic field, which means they can be guided effectively using a magnetic field gradient,

* Address correspondence to slavko.kralj@ijs.si.

Received for review April 18, 2015 and accepted September 22, 2015.

Published online September 22, 2015
10.1021/acsnano.5b02328

and, even more importantly, they quickly arrange into one-dimensional, chain-like structures when exposed to a homogeneous magnetic field.[20−22] The periodicity of this internal structure can be precisely tuned by the strength of the applied magnetic field. This effect is the basis for applications in magnetically tunable photonic crystals.[23−25]

The magnetic-field-assisted assembly of superparamagnetic particles in a suspension can also be applied for the syntheses of 1-D nanostructures, such as nanochains, nanorods, or peapod-like particles.[20,26−28] The anisotropy of their shape, their strong magnetic moment, and the regular periodicity of their structure (*i.e.*, the size of the primary SNCs in the nanochain and the defined spacing between the adjacent SNCs) give them many advantages in potential applications. In addition, the regular periodicity of the SNCs inside the nanochains can serve as a basic structural color unit for a new type of photonic inks.[29]

For the syntheses of the chain-like structures, the SNCs can be magnetically assembled into nanochains and simultaneously fixated by coating with a layer of silica, carbon, or titania to keep their structure permanent when the applied magnetic field is turned off.[26,27,30] Since the SNCs come into close proximity during the magnetic assembly, the periodicity of the 1-D structure can be easily determined by the size of the SNCs and the thickness of their primary coating. However, control of the nanochain length, defined by the number of SNCs in the nanochain, has remained a challenge, despite the significant progress in colloidal synthesis and processing over the past two decades.[26,31] In particular, the controlled direct synthesis of silica-fixated superparamagnetic nanochains with lengths shorter than 2 μm, containing only up to 20 SNCs per nanochain, appears to be relatively difficult. Moreover, combinations of magnetic-field-assisted dynamic assembly with flow-induced disassembly were rarely described in the scientific literature.[2] Ding and co-workers demonstrated advances in the fabrication of photonic crystals from magnetic ellipsoid particles with controlled solvent evaporation and magnetic-field-assisted particle deposition on a solid support.[32]

Here, we present a versatile and flexible approach based on the simultaneous magnetic assembly and stirring-induced disassembly of SNCs into nanochains and their bundles (nanobundles) followed by their fixation with an additional layer of deposited silica. The magnetic assembly of nanochains was stabilized by polyvinylpyrrolidone (PVP) and fixated by the deposition of an additional layer of silica using the controlled hydrolysis and condensation of tetraethoxysilane (TEOS). Our approach enables excellent length control for the shorter nanochains composed of up to ~20 SNCs, whereas the length control of the longer nanochains was less precise. The PVP stabilized the temporarily magnetically assembled nanochains in the suspension during stirring, which made it possible to fixate the nanochains by silica deposition. The nanochain length was controlled by the time for which the suspension was exposed to the magnetic field: longer periods of exposure to a magnetic field led to the formation of longer nanochains. Apart from the strength of the magnetic field and the SNC volume fraction, the important parameters for controlling the nanochain length are the concentration of PVP, the stirring rate, and the magnetic-field exposure time. An additional special advantage of our approach is the possibility to fine-tune the spacing between neighboring SNCs inside individual nanochains by controlling just the thickness of the SNCs' primary silica coating.

RESULTS AND DISCUSSION

The fabrication processes for the nanochains and nanobundles are schematically presented in Figure 1. Highly colloidally stable, aqueous suspensions of superparamagnetic maghemite (γ-Fe_2O_3) nanoparticle clusters with either 5 nm (SNC5) or 20 nm thick (SNC20) primary silica coatings were provided by Nanos SCI.

The average SNC size was determined from the transmission electron microscopy (TEM, Jeol, JEM 2100) images (Figure 2) to be 114 and 146 nm (Figure 2c,f) for the 5 nm and 20 nm thick silica shells, respectively. The SNCs showed superparamagnetic properties with a saturation magnetization M_S of ~45 A m^2 kg^{-1} and ~32.1 A m^2 kg^{-1} for SNC5 and SNC20, respectively, corresponding to ~68 wt % (SNC5) and ~49 wt % (SNC20) of the magnetic phase (the M_S of the maghemite nanoparticles used for the assembly of the SNCs was 66 A m^2 kg^{-1}). The density of the particles was estimated from their composition to be 4402 and 3248 kg/m^3 for the SNC5 and SNC20, respectively.

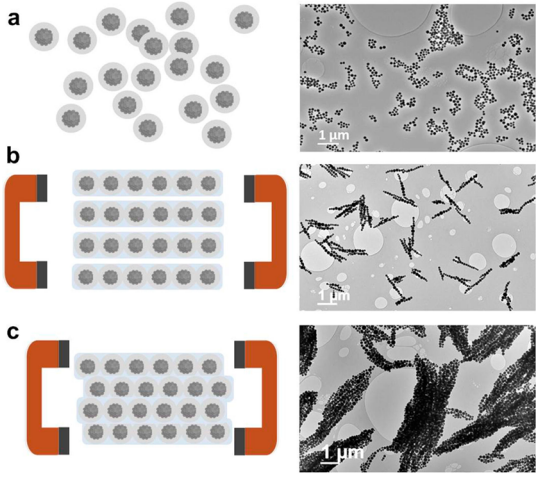

Figure 1. Schematic representation of the fabrication process (left-hand image) and the corresponding transmission electron microscopy images (right-hand image) of (a) silica-coated superparamagnetic nanoparticle clusters, (b) nanochains, and (c) nanobundles.

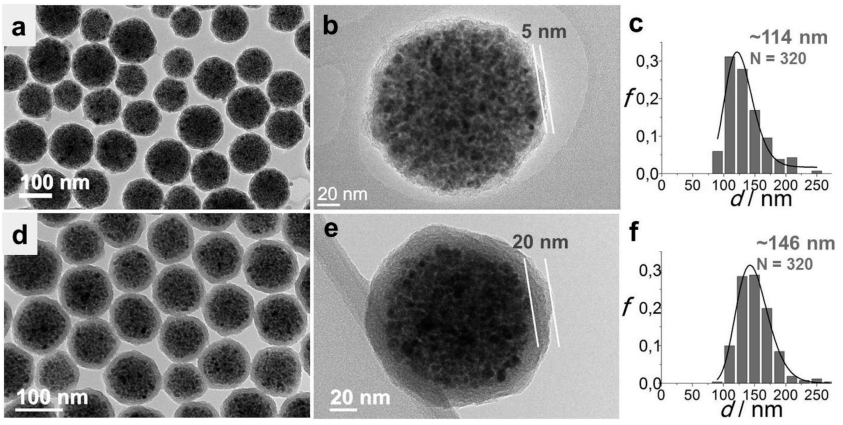

Figure 2. (a, b, d, and e) TEM images and the size distribution (the size expressed as an equivalent diameter was determined from the TEM images using DigitalMicrograph software) for the SNC5 nanoparticle clusters coated with (c) a 5 nm thick silica shell and the SNC20 with (f) a 20 nm thick silica shell.

First, the aqueous suspension of SNCs was transferred to the PVP solution and then exposed to a homogeneous magnetic field. Our experiments suggest that the macromolecules of the hydrophilic, neutral PVP polymer stabilize the structure of the magnetically assembled clusters, thereby decreasing the rate of disintegration due to stirring. The PVP-stabilized nanochain structures were permanently fixated with an additional layer of deposited silica, which is a product of the hydrolysis and condensation of TEOS in the presence of ammonia acting as the catalyst.

Under the influence of an applied magnetic field the SNCs in the suspension assemble into the chains due to magnetic dipole−dipole attractions. The maximum attraction of the magnetic dipolar interaction is described by a dimensionless dipole strength λ relative to the thermal energy (kT) disassembling the chains:

$$\frac{U_{max}}{kT} = -\lambda = \frac{\pi\mu_o\left(\frac{d}{2}\right)^3 H^2\chi^2}{9kT} \quad (1)$$

where U_{max} is a maximum potential energy of the interaction between two spheres with identical magnetic dipole moments in close contact aligned in the direction of the field, kT is the Boltzmann constant multiplied by the temperature, d is the cluster diameter, χ is the magnetic susceptibility, μ_o is the magnetic permeability of the vacuum, and H is the applied magnetic field.[33] The interaction thus scales with the square of the particles' magnetization ($M = \chi H$). Changing of the volume magnetization M_{vol} and the dipole strength λ with the applied H for the SNCs used is shown in Figure S1 (Supporting Information). Usually, λ with small values above 1 (typically 2−5) are already enough to assemble the magnetic particles into the chains. At higher values of λ the chains start to coalescence laterally to form bundles (columns, fibers).[33−37] The dominant mechanism for the chains' coalescence depends on several factors, including the volume fraction, the dipole strength, and the tendency of the system to form defects due to aggregation kinetics, particle polydispersity, roughness, or magnetic heterogeneity.[37]

During the fabrication of the nanochains and nanobundles the suspension was stirred. The stirring produces shear stress, continuously breaking the chains assembled by the magnetic dipolar interactions. The magnetically assembled chains break due to viscous forces, which are different for both ends of the chain subjected to a shear flow.[38]

In our first synthesis attempt, nanochains of uncontrolled lengths were formed most probably because the attractive magnetic dipolar interactions between the SNCs were induced by a weak and nonuniform magnetic field during conventional magnetic stirring (Supporting Information Figure S2). The magnetic field induced by the magnetic stirrer was a maximum of $\sim 1.6 \times 10^4$ A m^{-1}, corresponding to the dipole strength λ of 76 and 68 for SNC5 and SNC20, respectively, and the reaction mixture was exposed to the magnetic field for the whole 3 h (a typical time period for the complete synthesis process). The synthesis was carried out at a PVP concentration of 1.25×10^{-4} M and an SNC concentration of 1.6×10^{-8} M, corresponding to a volume fraction $\phi \approx 0.002$. First, the TEOS was slowly hydrolyzed at pH 4.3 for 90 min, and then the nucleation of the silica was initiated by the addition of diluted ammonia to set the pH to a value of ~8. Next, we systematically studied all the relevant factors influencing the fabrication of the nanostructures in the presence of a controlled and uniform magnetic field.

Impact of PVP. The PVP stabilized the temporarily magnetically assembled nanochains in the suspension during stirring, which made it possible to fixate the nanostructures by silica deposition. The stabilizing polymer was carefully chosen based on the expected interactions with the silica surface, depending on the reaction mixture's pH. The PVP was an ideal candidate since it forms relatively weak hydrogen bonds with

silica OH groups in moderately acidic media.[39] An increase in pH leads to the dissociation of the silica surface OH groups and a decreased potential for hydrogen bonding between the polymer and the surface. The silica OH groups became dissociated once the pH of the reaction mixture was increased, and this promotes continuous desorption of the PVP from the silica surfaces. Thus, the hydrolyzed silica precursors can be continuously deposited on the assembled structures in the form of a secondary layer of silica during the pH increase. In contrast, we found that the stronger electrostatic attractive interactions between the negatively charged silica surface and the cationic polyelectrolyte/surfactant poly(allylamine) (PAH) were not suitable for the stabilization of our system. The PAH of similar molecular weight to the PVP promoted the cross-linking of the SNCs due to strong attractive interactions, which leads to uncontrolled agglomeration. Anionic surfactants cannot be used for the stabilization of the suspension containing the particles with negatively charged silica surfaces. However, the anionic surfactants, such as poly(acrylic acid) (PAA), can be used for the stabilization of the iron-oxide magnetic nanoparticles without the silica shell. The PAA was thus successfully applied for the stabilization of the magnetic nanoparticles during their assembly in the form of filaments.[40]

The absence of PVP in the suspension impairs the colloidal stability during the sol−gel process, and the clusters tend to agglomerate permanently after increasing the pH with ammonia, which is necessary to catalyze the hydrolysis of the TEOS. PVP concentrations below 0.1×10^{-4} M led to an additional coating of SNCs and to their partial agglomeration (Supporting Information Figure S3), whereas concentrations of PVP higher than 3.7×10^{-4} M favored the homogeneous nucleation and growth of individual silica nanoparticles and an additional coating of primarily silica-coated clusters (Supporting Information Figure S4). This shows that the optimum PVP concentration is crucial for the preparation of well-defined nanochains.

Magnetic-Field Strength. The application of a magnetic field is needed to align the superparamagnetic clusters into nanochains. The magnetic-field strengths above approximately 8×10^3 A m^{-1}, corresponding to the dipole strengths λ of ~27 (SNC5) and ~16 (SNC20), effectively form the nanochains in the suspension with the volume fraction of SNCs $\phi = 0.002$. The value of λ is considerably larger than the usually reported values in the literature for magnetic dipolar assembly and reflects the influence of stirring, which continuously breaks the formed chains. However, the volume fraction was also considerably lower than those usually reported for the magnetic assembly of superparamagnetic particles into chains. Usually, the magnetic assembly of larger, micrometer-sized superparamagnetic particles in suspensions was studied on the basis of direct observations using optical microscopy.[33,37,41] Theoretically, the chains will form as soon as the magnetic dipole strength exceeds the thermal energy. Experimentally, Fermigier and Gast observed a saturation of the chain length at a dipole strength $\lambda = 4.5$ and a volume fraction $\phi = 0.005$ and at $\lambda = 2.2$ for the larger $\phi = 0.011$.[33]

The nanochains further evolved into nanobundles once the suspension ($\phi = 0.002$) was exposed to a stronger magnetic field of 8.8×10^4 A m^{-1}, but only for the SNC5 (dipole strength λ was 428). For the SNC20 the value of λ remained too low ($\lambda \approx 254$) for the lateral coalescence of the formed nanochains into the nanobundles. The magnetic field of 8.8×10^4 A m^{-1} was the highest uniform magnetic field that we can apply. If the magnetic field was further increased, a nonuniform product was formed because of the nonhomogeneity of the applied field. The mechanisms involved in the lateral coalescence of the chains were systematically presented by Furst and Gast.[37]

Duration of Magnetic-Field Exposure. The magnetically assembled nanochains should be preserved long enough for them to be fixated by the silica coating. The key to controlling the length of the synthesized nanochains is the duration of the reaction mixture's exposure to the magnetic field. The optimum magnetic-field exposure times for the SNC5 suspension ($H \approx 5.2 \times 10^4$ A m^{-1}, $\lambda \approx 284$, $\phi = 0.002$) were 85 and 120 min for the shortest nanochains (CHAINS 6) and medium nanochains (CHAINS 14) composed of ~6 and ~14 clusters per nanochain, respectively (Figure 3a,b,d,e). When the time of exposure to the magnetic field was longer than 3 h, an uncontrolled interchain silica bridging was frequently observed (Supporting Information Figure S5). Longer periods of exposure for the suspension containing SNC5 led to longer and less defined nanochains, whereas the exposures shorter than 1 h led to individual, additionally silica-coated SNCs, because the hydrolysis of the TEOS cannot be completed and not enough silica is deposited to fixate the temporarily assembled clusters into nanochains.

The length of the nanochains composed of SNC20 cannot be controlled as precisely as in the case of SNC5. The longer chains were fixated in the suspension of SNC20, where the dipole strength was considerably smaller ($\lambda \approx 176$), while all other parameters of the assembly remained unchanged. In the case of the SNC20 the length of the nanochains varied from 10 to 40 SNC20 per nanochain, irrespective of the field-exposure time (CHAINS L). Promislow and co-workers showed that the chain length s grows with a power-law dependence on time t ($s \sim t^z$). The power-law exponent z has a weak inverse dependence on both the volume fraction ϕ and the dipole strength λ.[41] Thus, with lower values of λ, larger chains are generally expected for a particular time of the magnetic assembly. However, the dipole strength λ has the opposite influence on the

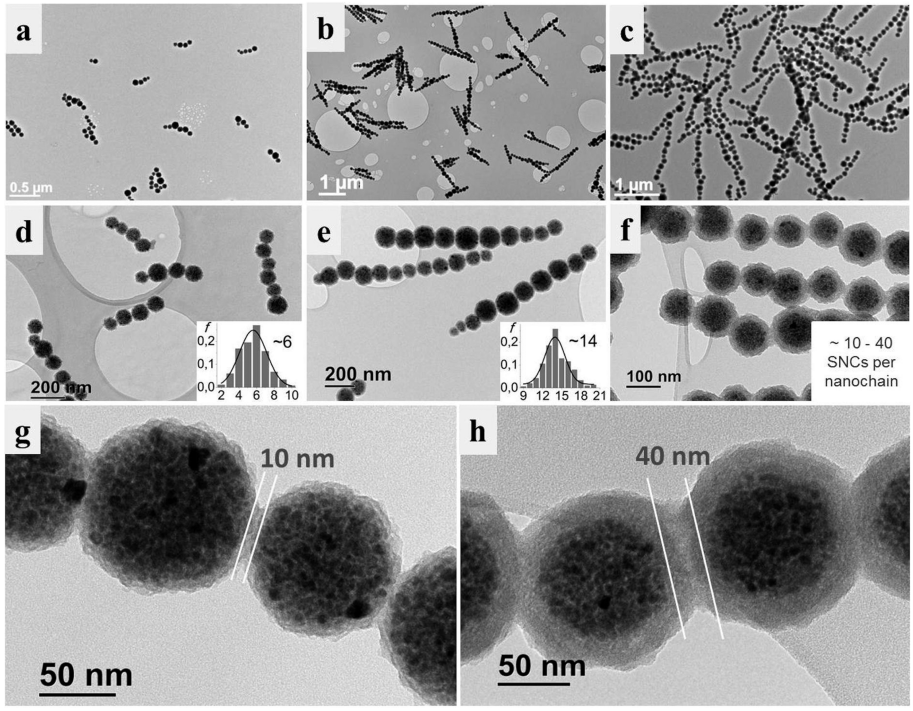

Figure 3. (a and d) TEM images of the CHAINS 6 composed of approximately six clusters, (b and e) TEM images of the CHAINS 14 composed of approximately 14 clusters, and (c and f) TEM images of CHAINS L composed of up to 40 clusters per nanochain. The insets in images (d), (e), and (f) show the length distributions of the nanochains determined by the manual counting of the clusters assembled into individual nanochains (80 nanochains counted for each sample). TEM images of typical nanochains composed of (g) SNC5 and (h) SNC20 show a defined spacing between the adjacent clusters in a nanochain of 10 or 40 nm, respectively.

stirring-induced disassembly. Under stirring the magnetically assembled chains will disassemble faster at lower values of λ.[38] While the length of the nanochains assembled in the suspension is determined by the processes of magnetic assembly and the stirring-induced disassembly, the final length of the synthesized nanochains additionally depends on the efficiency of the sol−gel process applied to permanently fixate the assembled structure. This process depends crucially on the colloidal properties of the suspension during the process of the secondary silica deposition, strongly influenced by use of the PVP surfactant.

Volume Fraction. Similarly, a low concentration (low volume fraction) of SNCs in the suspension made the formation of nanochains under a magnetic field practically impossible. Highly diluted SNC suspensions with concentrations lower than 0.4×10^{-9} M (volume fraction $\phi \approx 5 \times 10^{-5}$) cannot be used for the fabrication of permanent nanochains because the clusters are too far apart for an effective magnetic assembly into nanochains or because the assembled structures disintegrate before they are fixated by an additional layer of silica. SNC concentrations higher than 1×10^{-7} M (volume fraction $\phi \approx 1.25 \times 10^{-2}$) usually lead to nonuniform products composed of structures such as additionally silica-coated clusters, nanochains of various lengths, and larger, silica-connected clusters with undefined shapes. The rapid magnetic assembly of SNCs into nanochains is unaffected, even at a cluster concentration of 5×10^{-7} M (volume fraction $\phi \approx 6.25 \times 10^{-2}$).[37] These results suggest that the higher cluster density and the consequently reduced diffusion of the reactants limit the possibility for a controlled sol−gel synthesis. He and co-workers reported on the magnetic assembly of nonmagnetic polystyrene beads in ferrofluids where interesting phase evolutions of 1-D chain-like structures, 2-D labyrinth- and ribbon-like structures, and 3-D assemblies were observed at a high volume fraction $\phi \approx 0.04$.[42] Zhang and co-workers described a dynamic magnetic assembly process where 2-D labyrinth structures were fixated by silica.[34] These photonic structures were prepared at ~10 times higher volume fractions compared with the particle concentration used in our study.

Apart from the nanochain length, the distance between the SNCs inside an individual nanochain is important for applications in tunable photonic crystals. The intercluster distance is defined by the thickness of the primary silica shell of the SNCs. The SNC5- and SNC20-containing nanochains are formed with an intercluster distance of 10 nm (Figure 3g) and 40 nm (Figure 3h), respectively. If required, the synthesized nanochains can be additionally coated with an even thicker secondary silica shell (Supporting Information Figure S6).

Design of Nanobundles. The bundles of superparamagnetic nanochains (nanobundles) were formed when the

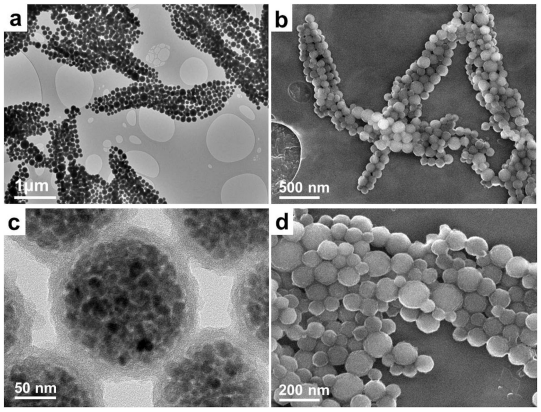

Figure 4. (a, c) TEM images and (b, d) SEM images of the basic type of nanobundles.

TEOS was first completely hydrolyzed under slightly acidic conditions, and then the silica was deposited at an increased pH using a small amount of ammonia (Figure 4). The reaction mixture containing SNC5 was exposed to a relatively strong magnetic field of 8.8×10^4 A m^{-1} ($\lambda \approx 428$) for 8 h after the addition of the TEOS. The chosen conditions for both the hydrolysis of the TEOS and the nucleation of silica were crucial for the cluster fixation into nanobundles. The hydrolysis of the TEOS was accelerated in an acidic medium at pH 2.9, followed by the nucleation of silica after the addition of a small amount of ammonia.

The formed nanobundles were approximately 1−2 μm wide and approximately 5−10 μm long and were composed of several primarily nanochains (Figure 4 a,b; see also Supporting Information Figure S7). In our basic experiment, TEOS, a silica precursor, was completely hydrolyzed before the final pH of the reaction mixture was set to 4.7 when the silica started to deposit. The silica nucleation and deposition at pH 4.7 are very slow, and it cannot be completely deposited even in a period of days. As a consequence, only a very small amount of added TEOS deposited as secondary silica connecting the assembled clusters into nanochains, and an even smaller amount of the secondary silica was deposited for further interchain connections (Figure 4c). To demonstrate the rigidity of the structures, the formed nanobundles were coated with an additional, third, layer of silica. TEM images showed that the nanobundles were completely coated with a thick silica layer (Supporting Information Figure S8). If the pH value of the reaction mixture was further increased to pH ~8, a large amount of silica was immediately deposited; however, nonuniform structures were formed due to uncontrolled agglomeration (Supporting Information Figure S9). In a special case, when both the hydrolysis of TEOS and the deposition of silica were performed at pH 8.5 (the pH was not primarily set to 2.9), the silica nucleation and deposition were significantly faster compared to acidic reaction conditions. As a result, the magnetically assembled structures were intensively

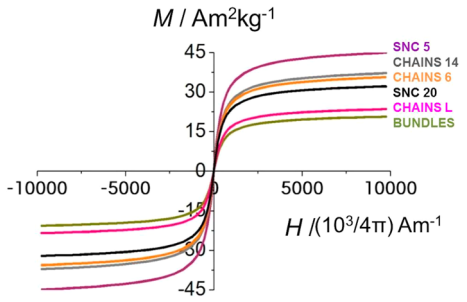

Figure 5. Room-temperature measurements of the mass magnetization as a function of magnetic field for the SNC5, SNC20, CHAINS 6, CHAINS 14, CHAINS L, and a basic type of nanobundles.

fixated by the deposition of the thicker layer of the secondary silica. However, in this case the nanobundles were narrower, typically composed of only a few nanochains, while the majority of the material remained in the form of separate nanochains (Supporting Information Figure S10c).

During the basic procedure of nanobundle synthesis the suspension was stirred at 250 rpm, which is the same stirring rate as applied for the preparation of all types of nanochains. When the synthesis of the nanobundles was carried out at the stirring rate of 750 rpm (all other parameters remained unchanged), the stirring-induced stresses intensively disintegrated the magnetically assembled structures, and thus only nanobundles composed of a few nanochains were formed (Supporting Information Figure S11).

Magnetic Properties. All the nanostructures show zero coercivity, which is in agreement with them having superparamagnetic properties at room temperature.[43] The nanochains and nanobundles preserve their superparamagnetism during the processing from the superparamagnetic clusters, which is an important advantage for their potential applications in biomedicine (Figure 5). There are no spontaneous magnetic dipole−dipole interactions between these nanostructures when the magnetic field is removed, which makes the preparation of stable colloidal suspensions less demanding. Suspensions containing nanobundles exhibit a good colloidal stability with a ζ-potential of more than −30 mV at pH values higher than 4, and they do not spontaneously sediment in 2 days.

CONCLUSION

In summary, we have developed a relatively simple, template-free, and low-cost fabrication approach for the direct synthesis of complex, well-defined, magnetically responsive nanostructures. Our magnetically responsive superparamagnetic nanostructures have a controlled aspect ratio, a uniform size, and a well-defined shape, and they express good colloidal stability. Our future research will focus on providing a proof-of-concept for a new cancer-treatment approach where nanochains are accumulated in the cancerous

tissue and used to mechanically damage cancerous cells by magnetically induced nanochain rotation. Such suspensions of synthesized materials can also have applications in magnetorheology.

METHODS

Preparation of SNCs. The SNC5 and SNC20 particles were provided by Nanos SCI (Nanos Scientificae Ltd.), commercially available under the "iNANOvative|silica cr" trademark. Their syntheses were based on the assembly of maghemite (γ-Fe_2O_3) nanoparticles with specially adjusted surface properties into the clusters in an emulsion system. Subsequently, the assembled nanoparticle clusters were coated with a silica shell.[44] The precise control of the clusters' size is obtained by size sorting using a high-gradient magnetic separator. The procedure is described in detail in Supporting Information S12.

Syntheses of Nanochains. First, the aqueous suspension of the silica-coated clusters was transferred into the PVP solution at pH 4.3. All the sol−gel mixtures were nonmagnetically stirred at 250 rpm during the syntheses.

Syntheses of CHAINS 6 and CHAINS 14. A typical synthesis for the short (CHAINS 6) and medium (CHAINS 14) nanochains was carried out at a PVP concentration of 1.25×10^{-4} M, with exposure to a magnetic field of $(5.2 \pm 1.2) \times 10^4$ A m^{-1} for 85 or 120 min after the addition of TEOS, a SNC5 concentration of 1.6×10^{-8} M, and a TEOS concentration of 60 mM. The TEOS was added 10 min after the transfer of the SNCs into the PVP solution. The pH value was set to 8.5, using 0.5% ammonia, after 80 min of TEOS addition.

Synthesis of CHAINS L. CHAINS L were prepared under the same conditions as CHAINS 6, but using the SNC20 instead of the SNC5 nanoparticle clusters. All the nanochain syntheses were completed in 3 h.

Synthesis of Nanobundles. The nanobundles were prepared from SNC5 in the following primary reaction mixture: 1.6×10^{-8} M SNC5, 60 mM TEOS, and 1.25×10^{-4} M PVP solution, adjusted to pH 2.9 using 0.1 M HBr. After the addition of the TEOS, the mixture was exposed to a magnetic field of $(8.8 \pm 1.6) \times 10^4$ A m^{-1} for 8 h. The pH value was increased twice, first to 4.2 using 0.5% ammonia, 4 h after the TEOS addition, and further to pH 4.7 using 0.1% ammonia, 6 h after TEOS addition. Finally, the synthesized nanochains and nanobundles were magnetically separated from the suspension and washed five times with distilled water.

Conflict of Interest: The authors declare no competing financial interest.

Supporting Information Available: The Supporting Information is available free of charge on the ACS Publications website at DOI: 10.1021/acsnano.5b02328.

Additional experimental details and TEM characterization (PDF)

Acknowledgment. The support of the Ministry of Higher Education, Science and Technology of the Republic of Slovenia within the National Research Program P2-0089 is gratefully acknowledged. We acknowledge the use of equipment in the Center of Excellence on Nanoscience and Nanotechnology−Nanocenter. The authors thank Asst. Prof. Darja Lisjak for the SEM analysis. The authors also thank U. Osolnik for determination of the cluster size distributions from the TEM images and B. Anželak for VSM measurements.

REFERENCES AND NOTES

1. Majetich, S. A.; Wen, T.; Booth, R. A. Functional Magnetic Nanoparticle Assemblies: Formation, Collective Behavior, and Future Directions. *ACS Nano* **2011**, *5*, 6081–6084.
2. Grzelczak, M.; Vermant, J.; Furst, E. M.; Liz-Marzan, L. M. Directed Self-Assembly of Nanoparticles. *ACS Nano* **2010**, *4*, 3591–3605.
3. Hickey, R. J.; Haynes, A. S.; Kikkawa, J. M.; Park, S. J. Controlling the Self-Assembly Structure of Magnetic Nanoparticles and Amphiphilic Block-Copolymers: From Micelles to Vesicles. *J. Am. Chem. Soc.* **2011**, *133*, 1517–1525.
4. Kavre, I.; Kostevc, G.; Kralj, S.; Vilfan, A.; Babič, D. Fabrication of Magneto-Responsive Microgears Based on Magnetic Nanoparticle Embedded PDMS. *RSC Adv.* **2014**, *4*, 38316–38322.
5. Yang, Y.; Gao, L.; Lopez, G. P.; Yellen, B. B. Tunable Assembly of Colloidal Crystal Alloys Using Magnetic Nanoparticle Fluids. *ACS Nano* **2013**, *7*, 2705–2716.
6. Di Corato, R.; Bigall, N. C.; Ragusa, A.; Dorfs, D.; Genovese, A.; Marotta, R.; Manna, L.; Pellegrino, T. Multifunctional Nanobeads Based on Quantum Dots and Magnetic Nanoparticles: Synthesis and Cancer Cell Targeting and Sorting. *ACS Nano* **2011**, *5*, 1109–1121.
7. Colombo, M.; Carregal-Romero, S.; Casula, M. F.; Gutierrez, L.; Morales, M. P.; Bohm, I. B.; Heverhagen, J. T.; Prosperi, D.; Parak, W. J. Biological Applications of Magnetic Nanoparticles. *Chem. Soc. Rev.* **2012**, *41*, 4306–4334.
8. Deng, Y.; Qi, D.; Deng, C.; Zhang, X.; Zhao, D. Superparamagnetic High-Magnetization Microspheres with an Fe_3O_4@SiO_2 Core and Perpendicularly Aligned Mesoporous SiO_2 Shell for Removal of Microcystins. *J. Am. Chem. Soc.* **2008**, *130*, 28–29.
9. Xu, X.; Friedman, G.; Humfeld, K. D.; Majetich, S. A.; Asher, S. A. Superparamagnetic Photonic Crystals. *Adv. Mater.* **2001**, *13*, 1681–1684.
10. Ge, J.; Hu, Y.; Yin, Y. Highly Tunable Superparamagnetic Colloidal Photonic Crystals. *Angew. Chem.* **2007**, *119*, 7572–7575.
11. Ge, J.; Yin, Y. Responsive Photonic Crystals. *Angew. Chem., Int. Ed.* **2011**, *50*, 1492–1522.
12. Singh, G.; Chan, H.; Baskin, A.; Gelman, E.; Repnin, N.; Kral, P.; Klajn, R. Self-Assembly of Magnetite Nanocubes into Helical Superstructures. *Science* **2014**, *345*, 1149–1153.
13. Nakata, K.; Hu, Y.; Uzun, O.; Bakr, O.; Stellacci, F. Chains of Superparamagnetic Nanoparticles. *Adv. Mater.* **2008**, *20*, 4294–4299.
14. Bishop, K. J. M.; Wilmer, C. E.; Soh, S.; Grzybowski, B. A. Nanoscale Forces and Their Uses in Self-Assembly. *Small* **2009**, *5*, 1600–1630.
15. Dušak, P.; Mertelj, A.; Kralj, S.; Makovec, D. Controlled Heteroaggregation of Two Types of Nanoparticles In an Aqueous Suspension. *J. Colloid Interface Sci.* **2015**, *438*, 235–243.
16. Erb, R. M.; Son, H. S.; Samanta, B.; Rotello, V. M.; Yellen, B. B. Magnetic assembly of colloidal superstructures with multipole symmetry. *Nature* **2009**, *457*, 999–1002.
17. Poselt, E.; Kloust, H.; Tromsdorf, U.; Janschel, M.; Hahn, C.; Maslo, C.; Weller, H. Relaxivity Optimization of a PEGylated Iron-Oxide-Based Negative Magnetic Resonance Contrast Agent for T_2-Weighted Spin-Echo Imaging. *ACS Nano* **2012**, *6*, 1619–1624.
18. Kralj, S.; Makovec, D. The Chemically Directed Assembly of Nanoparticle Clusters from Superparamagnetic Iron-Oxide Nanoparticles. *RSC Adv.* **2014**, *4*, 13167–13171.
19. Deng, Y.; Cai, Y.; Sun, Z.; Liu, J.; Liu, C.; Wei, J.; Li, W.; Liu, C.; Wang, Y.; Zhao, D. Multifunctional Mesoporous Composite Microspheres with Well-Designed Nanostructure: A Highly Integrated Catalyst System. *J. Am. Chem. Soc.* **2010**, *132*, 8466–8473.
20. Bannwarth, M. B.; Kazer, S. W.; Ulrich, S.; Glasser, G.; Crespy, D.; Landfester, K. Well-Defined Nanofibers with Tunable Morphology from Spherical Colloidal Building Blocks. *Angew. Chem., Int. Ed.* **2013**, *52*, 10107–10111.
21. Wang, M.; He, L.; Yin, Y. Magnetic Field Guided Colloidal Assembly. *Mater. Today* **2013**, *16*, 110–116.
22. Wang, X. Q.; Wang, C. F.; Zhou, Z. F.; Chen, S. Robust Mechanochromic Elastic One-Dimensional Photonic

Hydrogels for Touch Sensing and Flexible Displays. *Adv. Opt. Mater.* **2014**, *2*, 652–662.
23. Xuan, R.; Wu, Q.; Yin, Y.; Ge, J. Magnetically Assembled Photonic Crystal Film for Humidity Sensing. *J. Mater. Chem.* **2011**, *21*, 3672–3676.
24. Ge, J.; He, L.; Hu, Y.; Yin, Y. Magnetically Induced Colloidal Assembly into Field-Responsive Photonic Structures. *Nanoscale* **2011**, *3*, 177–183.
25. Velev, O. D.; Lenhoff, A. M.; Kaler, E. W. A Class of Microstructured Particles through Colloidal Crystallization. *Science* **2000**, *287*, 2240–2243.
26. Hu, Y.; He, L.; Yin, Y. Magnetically Responsive Photonic Nanochains. *Angew. Chem., Int. Ed.* **2011**, *50*, 3747–3750.
27. Ye, M.; Zorba, S.; He, L.; Hu, Y.; Maxwell, R. T.; Farah, C.; Zhang, Q.; Yin, Y. Self-Assembly of Superparamagnetic Magnetite Particles into Peapod-Like Structures and Their Application in Optical Modulation. *J. Mater. Chem.* **2010**, *20*, 7965–7969.
28. Smoukov, S. K.; Gangwal, S.; Marquez, M.; Velev, O. D. Reconfigurable Responsive Structures Assembled from Magnetic Janus Particles. *Soft Matter* **2009**, *5*, 1285–1292.
29. Wang, M.; He, L.; Hu, Y.; Yin, Y. Magnetically Rewritable Photonic Ink Based on Superparamagnetic Nanochains. *J. Mater. Chem. C* **2013**, *1*, 6151–6156.
30. Wang, H.; Chen, Q. W.; Sun, Y. B.; He, M. Y. Synthesis of Superparamagnetic Colloidal Nanochains as Magnetic-Responsive Bragg Reflectors. *J. Phys. Chem. C* **2010**, *114*, 19660–19666.
31. Wang, M.; He, L.; Zorba, S.; Yin, Y. Magnetically Actuated Liquid Crystals. *Nano Lett.* **2014**, *14*, 3966–3971.
32. Ding, T.; Song, K.; Clays, K.; Tung, C. Fabrication of 3D Photonic Crystals of Ellipsoids: Convective Self-Assembly in Magnetic Field. *Adv. Mater.* **2009**, *21*, 1936–1940.
33. Fermigier, M.; Gast, A. P. Structure Evolution in a Paramagnetic Latex Suspension. *J. Colloid Interface Sci.* **1992**, *154*, 522–539.
34. Zhang, Q.; Janner, M.; He, L.; Wang, M.; Hu, Y.; Lu, Y.; Yin, Y. Photonic Labyrinths: Two-Dimensional Dynamic Magnetic Assembly and *in Situ* Solidification. *Nano Lett.* **2013**, *13*, 1770–1775.
35. Islam, M. F.; Lin, K. H.; Lacoste, D.; Lubensky, T. C.; Yodh, A. G. Field-Induced Structures in Miscible Ferrofluid Suspensions With and Without Latex Spheres. *Phys. Rev. E: Stat. Phys., Plasmas, Fluids, Relat. Interdiscip. Top.* **2003**, *67*, 021402.
36. Laskar, J. M.; Philip, J.; Raj, B. Experimental Evidence for Reversible Zippering of Chains in Magnetic Nanofluids under External Magnetic Fields. *Phys. Rev. E* **2009**, *80*, 041401.
37. Furst, E. M.; Gast, A. P. Dynamics and Lateral Interactions of Dipolar Chains. *Phys. Rev. E: Stat. Phys., Plasmas, Fluids, Relat. Interdiscip. Top.* **2000**, *62*, 6916–6925.
38. Odenbach, S. *Magnetoviscous E□ects in Ferrofluids*; Springer-Verlag: Heidelberg, 2002.
39. de Vos, W. M.; Cattoz, B.; Avery, M. P.; Cosgrove, T.; Prescott, S. W. Adsorption and Surfactant-Mediated Desorption of Poly(vinylpyrrolidone) on Plasma- and Piranha-Cleaned Silica Surfaces. *Langmuir* **2014**, *30*, 8425–8431.
40. Goubault, C.; Jop, P.; Fermigier, M.; Baudry, J.; Bertrand, E.; Bibette, J. Flexible Magnetic Filaments as Micromechanical Sensors. *Phys. Rev. Lett.* **2003**, *91*, 260802.
41. Promislow, J. H. E.; Gast, A. P.; Fermigier, M. Aggregation Kinetics of Paramagnetic Colloidal Particles. *J. Chem. Phys.* **1995**, *102*, 5492–5498.
42. He, L.; Hu, Y.; Kim, H.; Ge, J.; Kwon, S.; Yin, Y. Magnetic Assembly of Nonmagnetic Particles into Photonic Crystal Structures. *Nano Lett.* **2010**, *10*, 4708–4714.
43. Tadic, M.; Kralj, S.; Jagodic, M.; Hanzel, D.; Makovec, D. Magnetic Properties of Novel Superparamagnetic Iron Oxide Nanoclusters and Their Peculiarity Under Annealing Treatment. *Appl. Surf. Sci.* **2014**, *322*, 255–264.
44. Kralj, S.; Makovec, D.; Čampelj, S.; Drofenik, M. Producing Ultra-Thin Silica Coatings on Iron-Oxide Nanoparticles to Improve their Surface Reactivity. *J. Magn. Magn. Mater.* **2010**, *322*, 1847–1853.